2019 10th International Power Electronics, Drive Systems and Technologies Conference (PEDSTC)
12-14 February, Shiraz University, Iran

A Fault-Tolerant Strategy for Three-Phase Dual Active Bridge Converter

Amirali Davoodi, Negar Noroozi, MohammadReza Zolghadri

Department of Electrical Engineering
Sharif University of Technology
Tehran, Iran

amirali.davoodi@gmail.com, nenoroozi@gmail.com, zolghadr@sharif.edu

***Abstract*—Due to several advantages, three-phase Dual Active Bridge (DAB) converter is widely used in numerous applications nowadays. On the other hand, this converter is very vulnerable to Transistor Open-Circuit Fault (TOCF). Therefore, a fault-tolerant (FT) scheme has been proposed in this paper to solve the problem. First, normal and faulty conditions are investigated, and according to the results, a fault-diagnosis (FD) approach is introduced. Using the outcomes of FD unit, a new post-fault strategy is proposed for the converter. The FD method is based on the DC component of transformer phase currents, and the basis of FT technique is shedding the faulty phase. Some benefits of the proposed scheme are preventing the shut-down of the system, no overvoltage or overcurrent, no additional power components, and insensitivity to operational conditions. Simulation results are also provided to confirm the analyses, and evaluate the performance of the proposed scheme.**

Index Terms – Fault-Tolerant Converters, Transistor Open-Circuit Fault, Fault-Diagnosis, Dual Active Bridge Converter

I. Introduction

Power electronic converters are used in many industries such as renewable energy systems, transportation, and aerospace. All these industries are striving to improve the reliability of the systems with cost-effective solutions. Additionally, apart from the human safety risks, failures in converters may lead to economic loss as a result of stoppage of the system as well as maintenance costs. As a solution for the problem, Fault-Tolerant (FT) converters have been proposed and become a wide research area in recent literature [1]. FT converters are proposed for a variety of applications, including an AC-AC converter [2], a multi-level converter in [3] and a quasi-Z-source inverter in [4]. Fault-Diagnosis (FD) techniques are the main part of the FT converters, which usually can identify the location of the fault [5]. Many FD methods are proposed for semiconductor faults [1]. Generally, after the detection of the fault, several post-fault strategies can be employed to guarantee the continuity of system operation in spite of the failure. Some of these strategies are as follows: redundancy, reconfiguration, and soft shutdown.

Furthermore, according to a survey about failed power converters, the most vulnerable components of a converter are power semiconductors. It is important to note that semiconductor faults account for 31% of failures in converter systems [1]. These faults are categorized into two main groups, including, short-circuit (SC) and open-circuit (OC) faults [1]. If not dealt with properly, both types can lead to serious damages. Typically, sufficient mechanisms are embedded in gate-drivers and power converters for SC protection. Unlike the SC fault, an OC fault usually remains undetected for a long time, deteriorating the performance of the system and can damage all the components. In addition, an OC fault in a power converter can occur as a result of the switch failure or a driver breakdown and it accounts for a large percent of semiconductor failures [6].

In addition, Dual Active Bridge (DAB), thanks to its numerous advantages, is extensively used in numerous applications. This converter has the benefits of high-power density, bidirectional power transfer, galvanic isolation, and so forth. All these benefits have paved the way for the usage of DAB in several applications, namely, electric vehicle, high-frequency-link power conversion systems, and battery storage systems [7]. Additionally, three-phase topology of the converter is usually preferred, in terms of efficiency and power-density, in industrial applications [8]. Having a large number of power semiconductors besides the corresponding gate-drivers, has made three-phase DAB seriously vulnerable to the power semiconductor failure. Even if a TOCF occurs in only one transistor of the converter, damage to other components, including 11 healthy switches, and the shutdown of the system will be unavoidable. Therefore, devising FD and FT techniques for this converter is necessary, in order to mitigate the consequence of TOCF and ensure the service continuity.

In [9], faults on DC buses are investigated and techniques for tackling this problem is proposed. In [10]-[11], the effect of transistor failures on the performance of the system is studied and FD techniques are presented, based on the voltage of the switches and transformer currents. In this paper a fault-tolerant scheme for three-phase DAB is introduced for the first time. This FT scheme includes an FD method for TOCF detection, and using the outputs of FD unit, a post-fault control strategy is presented. The FD approach is based on the DC component of transformer phase currents. As a result, the method has the minimum sensitivity to system parameters and operational conditions. Moreover, no additional power component is added and no extra consideration must be given concerning the current and voltage ratings of the switches. This scheme prevents not only the system shut-down but also the transformer saturation and damage to power semiconductors. In section II the converter is analyzed in normal condition. In section III, the effects of TOCF on the performance of the converter is studied and its main feature is extracted. Section IV introduces the proposed FD and FT techniques in detail. Section V presents the simulation results to confirm the analysis and prove the efficacy of the techniques.

978-1-5386-9254-7/19/$31.00 ©2019 IEEE

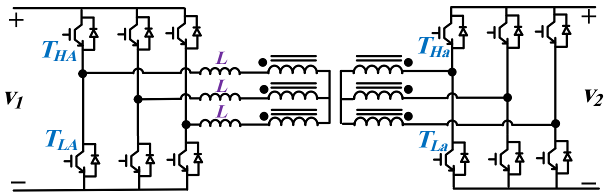

Fig. 1. Electrical schematic of a typical three-phase DAB converter

II. Principle of Operation

As shown in Fig. 1, the three-phase Dual Active Bridge (DAB) converter comprises two full-bridges (each containing 3 legs) connected together via a high-frequency three-phase transformer. In the understudy converter, the transformer windings are connected YY.

This converter is a DC-DC converter with the key advantage of bidirectional power transfer capability. In addition, it enjoys the benefits, including, high power density, soft-switching, galvanic isolation, and so forth. That means that the converter is suitable for a variety of applications [7]. In addition, its three-phase topology, due to lower stresses on power semiconductors, is more appropriate for industrial applications.

Additionally, the most common control strategy for the converter is single phase-shift (SPS) [13]. In SPS, in each bridge, the switching commands of three legs have $120°$ phase-shift with one another. Moreover, there is a main phase-shift ϕ, between the commands of one leg with its counterpart in the other bridge. By controlling ϕ, the magnitude and direction of the power transferred between legs can be controlled. In other words, in SPS, two bridges apply a symmetrical three-phase voltage across the equivalent leakage inductances of the transformer. Hence, the leakage inductances of the transformer will act similar to a transmission line between two bridges, and therefore, the power is transferred between bridges as a result of the phase-shift between three-phase voltages. The relationship between the transferred power P and phase-shift ϕ is according to (1), and the power flows form the leading bridge to lagging bridge [13]. In this equation, n is the turn ratio of the transformer, V_1 and V_2 are primary- and secondary-side bridge input and output DC voltage, L is the equivalent leakage inductance of each phase, and f_s is the switching frequency.

$$\begin{cases} P = \frac{nV_1V_2}{2\pi f_s L}\,\phi\left(\frac{2}{3} - \frac{\phi}{2\pi}\right), \ 0 < \phi < \frac{\pi}{3} \\ P = \frac{nV_1V_2}{2\pi f_s L}\left(\phi - \frac{\phi^2}{\pi} - \frac{\pi}{18}\right), \ \frac{\pi}{3} < \phi < \frac{2\pi}{3} \end{cases} \quad (1)$$

The normal operation of the three-phase DAB is extensively studied in [12]. The waveforms of the phase currents of the transformer in normal condition are shown in Fig. 2. As can be seen in this figure, no DC component exists in the currents during normal operation. Similarly, since the magnetization inductance of the transformer is located in the parallel branch, the DC component of the magnetization current must be zero too.

III. Open-Circuit Fault Analysis

Fig. 3 (a) shows a leg of the converter in healthy condition. As discussed in section II, in normal operation, during a half of the switching period, depending on the current direction, the current passes through high-side transistor or diode; during the other half of the switching period, the low-side transistor or diode must conduct the current.

Therefore, when all 12 switches in three-phase DAB-IBDC are healthy, once the command is properly given to a switch, the current can flow through the switch, irrespective of its direction. In contrast, when a TOCF occurs in one of the transistors of the leg, the flow of the current encounters a problem and will be dependent on its direction. For example, if TOCF happens in T_L, the equivalent circuit of the leg will be according to Fig. 3 (b). In this situation, if the command of the high-side switch is set, the current will pass through T_H or D_H similar to the normal condition. Likewise, if the command of high-side switch is cleared, and the low-side command is set while $i_{ph} > 0$ the current will pass through D_L as expected. On the contrary, if the current direction changes and $i_{ph} < 0$, since T_L is open-circuit and there is no conduction path in the low-side switch, the current must flow over the diode of the high-side switch, D_H. Similarly, in case of TOCF occurrence in T_H, the i_{ph} with positive value must pass through D_L inevitably. Accordingly, in case of TOCF in a switch, while the flow of the current through that switch is expected, the current will pass through the diode of the other switch at the same leg. As a result, anomalies will be seen in the converter performance. For example, in Fig. 1 if TOCF occurs in the low-side transistor of phase A, T_{LA}, and the low-side switch command is set, during some intervals, while $v_{AP} = 0$ is expected, the $v_{AP} = V_1$ will be the result. Similarly, a failure in T_{HA}, while its command is set, will result in v_{AP} =0, whereas $v_{AP} = V_1$ is expected normally. Such anomalies in voltages, including v_{AP}, v_{BP}, v_{CP}, v_{ap}, v_{bp}, v_{cp} , can lead to transformer saturation and power semiconductors overcurrent which will be elaborated hereunder. Regarding Fig. 4, which shows the equivalent circuit of the high-frequency transformer of three-phase DAB-IBDC

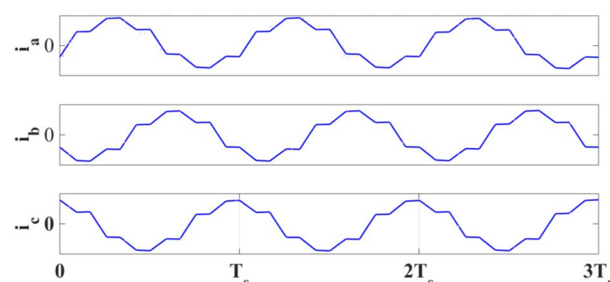

Fig. 2. Phase current waveforms in normal operation.

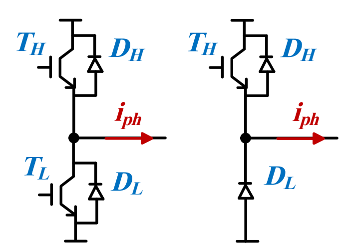

(a) (b)

Fig. 3. A leg of the converter. (a) Healthy state. (b) TOCF

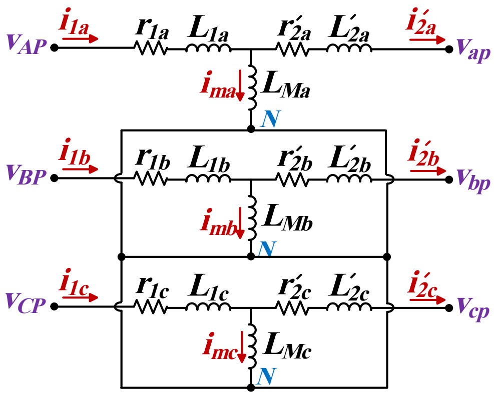

Fig. 4. Accurate equivalent circuit of the high-frequency transformer

referred to the primary-side, and using KVL as well as KCL, it can be written that:

$$\begin{cases} v_{AP} - v_N = \frac{2}{3}v_{AP} - \frac{1}{3}(v_{BP} + v_{CP}) \\ v_{BP} - v_N = \frac{2}{3}v_{BP} - \frac{1}{3}(v_{AP} + v_{CP}) \\ v_{CP} - v_N = \frac{2}{3}v_{CP} - \frac{1}{3}(v_{BP} + v_{AP}) \end{cases} \quad (2)$$

$$\begin{cases} v_{ap} - v_N = \frac{2}{3}v_{ap} - \frac{1}{3}(v_{bp} + v_{cp}) \\ v_{bp} - v_N = \frac{2}{3}v_{bp} - \frac{1}{3}(v_{ap} + v_{cp}) \\ v_{cp} - v_N = \frac{2}{3}v_{cp} - \frac{1}{3}(v_{bp} + v_{cp}) \end{cases} \quad (3)$$

Considering $r_1 = r_2 = r$, the DC component of primary, secondary, and magnetization current are as follows:

$$\begin{cases} i_{1kDC} = \frac{v_{KP} - V_N}{r} \\ i'_{2kDC} = -\frac{v_{kP} - V_N}{r} \\ i_{mkDC} = i_{1kDC} - i'_{2kDC} \\ \quad k = a, b, c \end{cases} \quad (4)$$

As calculated in (4), the DC component of magnetization current in each phase is a function of the DC component of voltages v_{AP}, v_{BP}, v_{CP}, v_{ap}, v_{bp}, v_{cp}. In healthy state, the overall DC component of the magnetization current is equal to zero. Any deviation in the DC component of the aforementioned voltages can upset the balance of (4),(3) and (2), and leads to a non-zero magnetization current DC component. It is worth mentioning that even small changes in the DC components of those voltages can result in substantial changes in magnetization current DC component, because the denominator r in (4) is a parasitic resistance and its value is typically very small. Moreover, in case of fault in the primary-side bridge, if the failure is in the transistor of high-side switch of phases A or B or C, the value of the DC component of the v_{AP} or v_{BP} or v_{CP} voltages decreases respectively. According to (4), (3), and (4), that will bring about a negative DC component in the magnetization current of the faulty phase and a positive DC component in the magnetization current of two healthy phases. In a similar way, the decrease in the DC component of v_{ap} or v_{bp} or v_{cp} voltages, as a result of the failure in high-side transistors of phases A or B or C of the receiver bridge, will lead to a negative DC component for the magnetization current of the faulty phase and a positive one for two healthy phases. By contrast, a fault in low-side transistors will act conversely, that is, a positive DC component for the faulty phase and a negative one for two defectless phases.

As previously mentioned, due to the small value of parasitic resistances, these DC components are generally considerable and will shift the operation point of the transformer. In other words, considering the nonlinear nature of the B-H curve of the core of transformer, the shift in operational point will lead the transformer to operate in the nonlinear part of the B-H curve rather than working in its linear zone. Consequently, not only do the DC component itself increase the rms values of the currents but also the saturation of the transformer worsens the condition. Hence, the rms values of the currents increase, and it poses serious risks on other power semiconductors and the transformer.

According to (3) and (4), in case of fault in the bridge of primary side, the DC component of the secondary currents i_{2a}, i_{2b}, i_{2c} decays over time and only the DC component of the primary side will remain. Likewise, failure in the bridge of secondary side, causes a decaying DC component in primary currents i_{1a}, i_{1b}, i_{1c} and non-decaying DC components in secondary currents. As a result, in fault condition, the DC component of either primary or secondary current is decaying and becomes zero with the passage of time. Therefore, i_{ph} for each phase is defined as the sum of primary and secondary currents of that phase, as can be seen in (5), so that the existence of DC component on i_{ph} is ensured during fault condition. Regarding (2), (3), (4) and (5) the polarity of DC component of i_{ph} for phase A is extracted in different transistor failure conditions, and tabulated in Table I.

$$i_{kphDC} = i_{1kDC} + ni'_{2kDC} \quad , \ k = a, b, c \quad (5)$$

IV. Fault-Diagnosis and Post-Fault Operation

A. Fault-Diagnosis

The basis of the proposed fault-tolerant three phase DAB-IBDC is diagnosis and deactivation of the faulty phase. In other words, the phase in which the failed transistor is located is recognized and subsequent decisions are made for post-fault control strategy accordingly. In this subsection, the approach for diagnosing the faulty phase will be introduced, and in next subsection the aforementioned decisions are described and post-fault control strategy will be elaborated upon.

In this paper, for diagnostic purposes, the focus will be on the polarity of the DC component of i_{ph}, which its

TABLE I
Polarity of the DC Component of i_{ph} in Different Transistor Failures in Phase A

Faulty Transistor	T_{HA}	T_{LA}	T_{Ha}	T_{La}
Polarity of i_{aphDC}	N	P	P	N
Polarity of i_{bphDC}	P	N	N	P
Polarity of i_{cphDC}	P	N	N	P

P: Positive, N: Negative

characteristics were investigated in previous section. In normal condition, with respect to (2)-(5), the DC component of i_{ph} is negligible and equal to zero. Hence, if the magnitude of the DC component of i_{ph} is a considerable non-zero value, the fault is detected. Additionally, according to table I, regardless of high-side or low-side location of the faulty transistor, the polarity of the DC component of i_{ph} of two healthy phases are identical to each other and opposite of faulty phase. Therefore, the faulty phase can be identified using this feature.

The block diagram of the proposed method for diagnosing the faulty phase is illustrated in Fig. 5. For each phase of the transformer, the secondary current and the primary current (referred to the secondary side) are added to form i_{ph}. Afterwards, in order to extract the magnitude of its DC component, i_{ph} passes through a low-pass filter. Then, the signal enters the polarity detector block. In this block, the input is compared to a positive and a negative threshold value. In case of being greater than the value, the polarity of input signal is detected as positive. Similarly, if the input signal is less than the negative threshold value, the polarity of signal is considered negative. Once the polarity of the DC components of i_{ph} is determined for each phase of the transformer, using the feature explained above, the fault is detected and the phase in which the fault has occurred is identified. By diagnosing the faulty phase, appropriate post-fault control strategy is chosen, which will be described as follows.

B. Post-Fault Operation

Immediately after diagnosing the faulty phase, all the switching commands to that phase are cleared—that is, all four switches of the faulty phase are forced to be turned off. Furthermore, the phase-shift between two remaining healthy phases, which was 120° before the fault occurrence, becomes 180° after identifying the faulty phase. That is to say, once the failure in one phase is detected, in each bridge, the leg associated with the faulty phase is put aside, and the phase shift between the legs of the defectless phases changes from 120° to 180°. In other words, three-phase DAB-IBDC will operate in single-phase mode after the TOCF.

It is worth mentioning that although the switching commands of the faulty phase are cleared immediately, the transformer phase current of that phase does not plunge to zero abruptly. If the transformer phase current (which is equal to the current passing through leakage inductance) falls suddenly to zero, due to the high value of di/dt, the resultant overvoltage across the leakage inductance could damage the transformer and power semiconductors. However, thanks to the presence of the antiparallel diodes in every switch, this phenomenon does not happen in the proposed post-fault control strategy. In spite of the turn-off command to the switches of the faulty phase, antiparallel diodes of the switches still provide a conduction path for the leakage inductance current. As a result, the current maintains its normal value until it becomes zero and all the diodes are turned off. Thus, the leakage inductance current becomes zero smoothly and no overvoltage will occur.

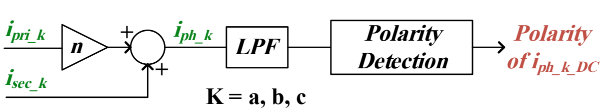

Fig. 5. Fault-diagnosis unit block diagram

Additionally, before the TOCF, (1) is true for the transferred power and the switches RMS current is calculated in [12]. After the occurrence of the failure, the transferred power and switches RMS current are calculated according to (7), [12]- [13]:

$$\begin{cases} I_{sw1RMS} = \frac{1}{2\sqrt{2}f_s(2L)}\sqrt{\frac{1}{12}(V_1^2+(nV_2)^2)+\frac{nV_1V_2}{3}e_{RMS}} \\ e_{RMS} = (1-\frac{2\phi}{\pi})(-\frac{1}{2}-\frac{\phi}{\pi}+\frac{\phi^2}{\pi^2}) \end{cases} \quad (6)$$

$$P = \frac{nV_1V_2\phi(\pi-\phi)}{2\pi^2 f_s(2L)} \quad (7)$$

It is important to note that in post-fault operation, since the leakage inductance of two healthy phases are in series with each other, the equivalent leakage inductance is twice the leakage inductance of each phase, and 2L in (6) and (7) is due to this fact. Fig. 6, drawn using (1) and (7), illustrates the transferable power in pre-fault and post-fault conditions in terms of the phase-shift ϕ between the bridges. In this figure, the values of transferred powers are normalized according to the maximum transferrable power in pre-fault condition. The value of maximum transferrable power in pre-fault condition, P_{max}, is calculated in (8). Regarding this figure and (7), if the transferred power before the fault occurrence is less than $9/14P_{max}$, in the post-fault operation, the converter can sustain this power by increasing the phase-shift ϕ. On the other hand, if the power is greater than $9/14P_{max}$ and less than P_{max}. The phase-shift ϕ must be set to $\pi/2$ and the maximum transferrable power in post-fault operation will be equal to $9/14P_{max}$.

$$P_{max} = \frac{7nV_1V_2}{72f_sL} \quad (8)$$

Moreover, the RMS value of switch currents in both post- and pre-fault states are shown in Fig. 7. This figure is obtained using [12] and (6), and based on parameters listed in table II. This figure shows the RMS value of the current passing through the each available switch in post- and pre-fault states. As can be seen in the figure, two curves are very similar. In other words, the RMS current of the switches in post-fault operation does not exceed that of the pre-fault sate, that is, the converter can operate in post-fault condition without any unbearable overcurrent.

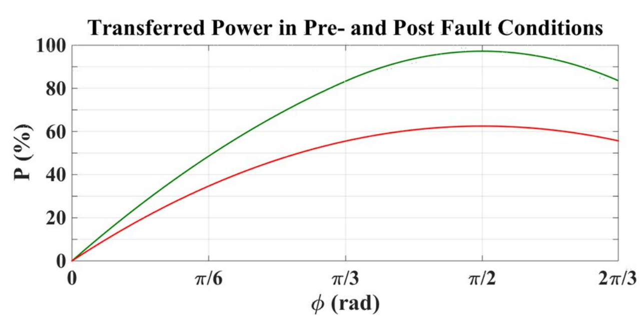

Fig. 6. Transferrable power in terms of ϕ in post-fault (red) and pre-fault (green) conditions

TABLE II
THE UNDERSTUDY CONVERTER PARAMETERS

Quantity	Symbol	Value
Transformer turn ratio	n	2
Input DC voltage	V_1	100 V
Output DC voltage	V_2	50 V
Switching frequency	f_s	25 kHz
Per-phase equiv. leakage inductance of the trans.	L	50 μH

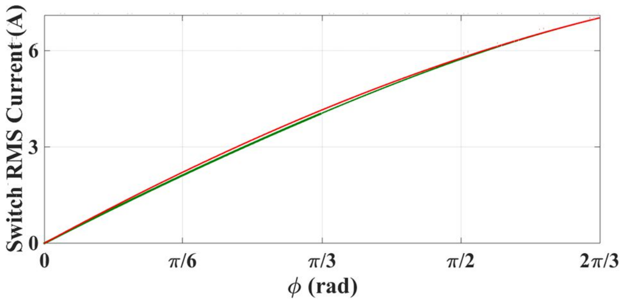

Fig. 7. RMS currents of the switches in terms of ϕ in post-fault (red) and pre-fault (green) conditions

V. SIMULATION RESULTS

In order to verify previous analyses, and assess the post-fault control strategy, the three-phase DAB illustrated in Fig. 1 with parameters shown in Table. II is simulated in MATLAB Simulink, and the results are presented in this section.

First, the ordinary three-phase DAB is simulated to investigate the consequences of TOCF for the converter. The transferred power is controlled through the closed-loop controller. The feedback from measured power is subtracted from setpoint power and is given to a PI controller.

While the transferred power is equal to 400W, a TOCF occurs at moment t=0.01s in the high-side switch of primary-side bridge in phase C. Fig. 8 shows the aforementioned i_{ph} for each phase. Evidently, a negative DC component for phase C (faulty phase), and positive DC components for phases A and B appear in i_{ph} once the fault occurs. In addition, the emerged DC components in magnetization currents can be seen in Fig. 9, which can result in transformer saturation.

On the other hand, when the similar simulation is undertaken while the fault-tolerant scheme is activated, as shown in Fig. 10, the zero DC component of the phase and magnetization currents of phases persists even after the occurrence of TOCF. The maximum transferrable power and

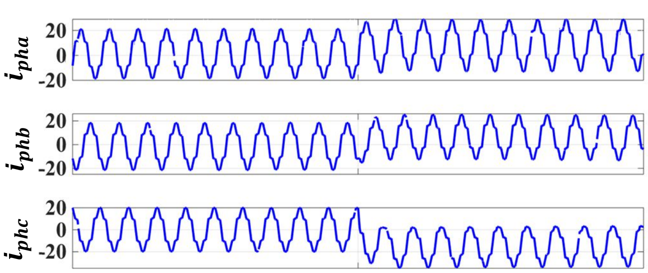

$T_F = 0.01\ (sec)$

Fig. 8. Behavior of i_{ph} of each phase, in case of TOCF in high-side switch of primary-side bridge in absence of fault-tolerant scheme.

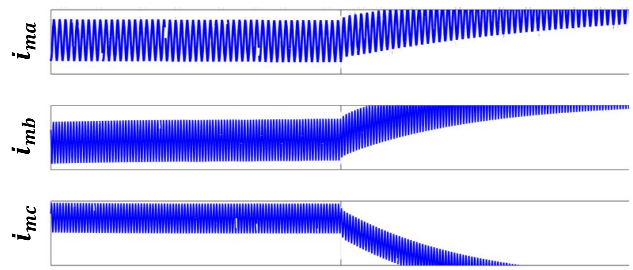

$T_F = 0.01\ (sec)$

Fig. 9. Appearance of DC component in magnetization currents, in case of TOCF in high-side switch of primary-side bridge in absence of fault-tolerant scheme

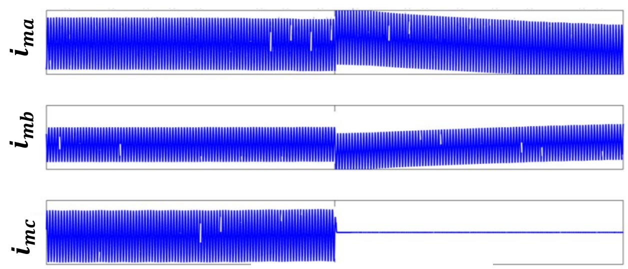

$T_F = 0.01\ (sec)$

Fig. 10. Proficiency of the Fault-tolerant scheme in avoiding transformer saturation through mitigating the DC component of the magnetization current.

TABLE III
MAXIMUM TRANSFERRABLE POWER (P) AND RMS OF SWITCH CURRENTS ($I_{RMS,sw}$) IN POST- AND PRE-FAULT STATES

	Pre-fault	Post-fault
P	697 W	447 W
$I_{RMS,sw}$	8.3 A	6.8 A

the maximum RMS of the switch currents, before and after the TOCF, are tabulated in Table. III. In this regard, and according to Fig. 11, the converter can transfer the 400W power despite the existence of TOCF while the RMS of the switch currents do not exceed the maximum value shown in Table III. Additionally, the output of fault-diagnosis is shown in Fig. 12. As can be seen in this figure, the fault-diagnosis block, identifies the faulty phase immediately after the occurrence of the TOCF, which proves the viability of this scheme.

VI. Conclusion

In this paper, an approach is proposed in order to make three-phase Dual Active Bridge converter tolerant of transistor

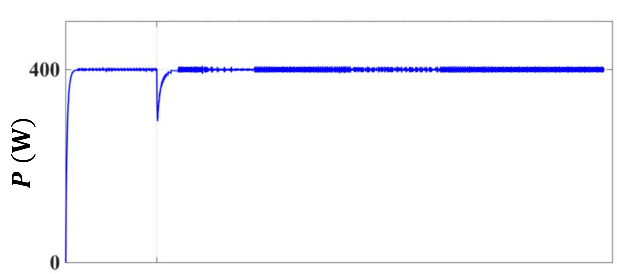

$T_F = 0.01\ (sec)$

Fig. 11. Maintaining the output power in spite of TOCF.

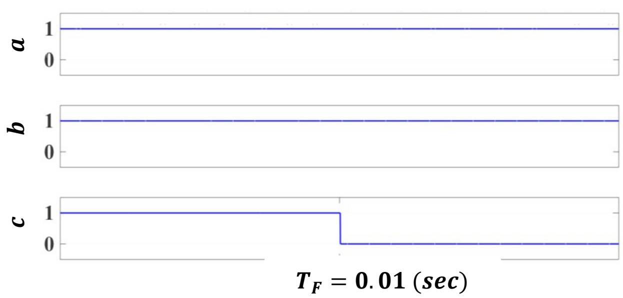

Fig. 12. Successful identification of faulty phase

open-circuit fault (TOCF). First, the converter is analysed under the condition of TOCF occurrence, and the consequences and features of the fault are extracted. As a result, the phase of the converter in which the TOCF has occurred is identified using the DC components of the phase currents of the high-frequency transformer. Subsequently, the switching commands to the faulty phase are disabled and the converter operational mode changes from three-phase to single-phase. The proposed scheme can maintain the power transferred between the bridges to an acceptable extent without additional considerations for the voltage or currents ratings of the power semiconductors. It is worth mentioning that without this scheme, a TOCF will result in transformer saturation, damage to power semiconductors, and eventually the shut-down of the system. Some other advantages of the proposed approach are simple implementation, insensitivity to the operational condition as well as parasitic elements. Finally, the accomplishment of the approach and analyses is verified through simulation of the converter in a TOCF condition.

References

[1] U. Choi, F. Blaabjerg and K. Lee, "Study and handling methods of power IGBT module failures in power electronic converter systems," in *IEEE Transactions on Power Electronics,* vol. 30, no. 5, pp. 2517-2533, 2015.

[2] M. Khodabandeh, M. R. Zolghadri, M. Shahbazi and N. Noroozi, "T-type direct AC/AC converter structure," in *IET Power Electronics*, vol. 9, no. 7, pp. 1426-1436, 2016.

[3] B. Li, S. Shi, B. Wang, G. Wang, W. Wang and D. Xu, "Fault diagnosis and tolerant control of single IGBT open-circuit failure in modular multilevel converters," in *IEEE Transactions on Power Electronics*, vol. 31, no. 4, pp. 3165-3176, April 2016.

[4] M. Yaghoubi, J. S. Moghani, N. Noroozi and M. R. Zolghadri, "IGBT Open-Circuit Fault Diagnosis in a Quasi-Z-Source Inverter," in *IEEE Transactions on Industrial Electronics*. doi: 10.1109/TIE.2018.2847709

[5] C. Shu, L. Wei, D. Rong-Jun and C. Te-Fang, "Fault diagnosis and fault-tolerant control scheme for open-circuit faults in three-stepped bridge converters," *in IEEE Transactions on Power Electronics*, vol. 32, no. 3, pp. 2203-2214, March 2017.

[6] L. M. A. Caseiro and A. M. S. Mendes, "Real-Time IGBT Open-Circuit Fault Diagnosis in Three-Level Neutral-Point-Clamped Voltage-Source Rectifiers Based on Instant Voltage Error," in *IEEE Transactions on Industrial Electronics*, vol. 62, no. 3, pp. 1669-1678, March 2015.

[7] B. Zhao, Q. Song, W. Liu and Y. Sun, "Overview of Dual-Active-Bridge Isolated Bidirectional DC–DC Converter for High-Frequency-Link Power-Conversion System", *IEEE Transactions on Power Electronics*, vol. 29, no. 8, pp. 4091-4106, 2014.

[8] T. Jimichi, M. Kaymak and R. De Doncker, "Comparison of single-phase and three-phase dual-active bridge DC-DC converters with various semiconductor devices for offshore wind turbines", *2017 IEEE 3rd International Future Energy Electronics Conference and ECCE Asia (IFEEC 2017 - ECCE Asia)*, 2017.

[9] Y. Shi and H. Li, "A novel modular dual-active-bridge (MDAB) dc-dc converter with dc fault ride-through capability for battery energy storage systems", *2016 IEEE Energy Conversion Congress and Exposition (ECCE)*, 2016.

[10] A. Airabella, L. Piris-Botalla, C. Falco, G. García and G. Oggier, "Semi-conductors faults analysis in dual active bridge DC–DC converter", *IET Power Electronics,* vol. 9, no. 6, pp. 1103-1110, 2016.

[11] A. Davoodi, D. Sadeghpour, M. Kashif, SA. Albahrani, M. Atarodi, MR Zolghadri, " A Novel Transistor Open-Circuit Fault Localization Scheme for Three-Phase Dual Active Bridge" *2018 Australian Universities Power Electronic Conference (AUPEC 2018)*, 2018.

[12] R. De Doncker, D. Divan and M. Kheraluwala, "A three-phase soft-switched high-power-density DC/DC converter for high-power applications", *IEEE Transactions on Industry Applications*, vol. 27, no. 1, pp. 63-73, 1991.

[13] F. Krismer, "Modeling and Optimization of Bidirectional Dual Active Bridge DC-DC Converter Topologies", Doctor of Science, ETH Zurich, 2010.